Volume 1 | Number 1 | Jan 2013 | Pages 1–100

Polymer Chemistry

www.rsc.org/polymers

ROYAL SOCIETY OF CHEMISTRY

ROYAL SOCIETY OF CHEMISTRY

www.rsc.org/polymers

Journal Name

ARTICLE

Preferential chiral solvation induced supramolecular chirality in optically inactive star Azo polymers: photocontrollability, chiral amplification and topological effect

Lu Yin, Yin Zhao, Shunqin Jiang, Laibing Wang, Zhengbiao Zhang, Jian Zhu, Wei Zhang* and Xiulin Zhu

A series of star–shaped azobenzene(Azo)–containing side chain polymers with 3, 4 and 6 arms were synthesized by atom transfer radical polymerization technique initiated by multifunctional initiators. The intense bisignated circular dichroism (CD) signals in the UV–vis region were observed when these star polymers aggregated in dichloroethane/limonene mixed solvent, indicating the successful chirality transfer from limonene molecules to these star Azo polymers. The chirality origates from the preferential supramolecular chirality of well–organized optically inactive side–chain Azo units. The supramolecular chirality is closely related to the volume fraction of cosolvents, the enantiopurity (*ee*) of limonene, molecular weight and arm numbers of star Azo polymers. Interestingly, the maximum values of CD and g_{CD} of the polymer aggregates increase with molecular weight in case of 3–armed Azo polymers, and increase simultaneously with arm numbers of the polymers having similar repeating units in each optimized experimental condition. Surprisingly, the first chiral amplification behaviours were observed in the 4– and 6–armed Azo polymers, but absence in linear and 3–armed counterparts. The supramolecular chirality can be destroyed by *trans–cis* photoisomerization and recovered by thermal *cis–trans* isomerization of Azo units. The current research will provide further insight into the mechanism study and production of effective chiroptical materials in chiral solvation induced supramolecular chirality of the achiral polymers.

Introduction

Supramolecular chirality has attracted significant attention due to not only a prime importance in living system but also potential applications in chiral sensors, chiroptical switches, chiral recognition and asymmetric catalysis.[1] In most cases, supramolecular chirality can be constructed from chiral building blocks by means of the non–covalent weak interactions, such as π–π stacking, hydrogen bonding, ionic interactions, van der Waals force and so on. Indeed, this strategy needs tedious procedures for synthesizing chiral building blocks with high enantiopurity (*ee*). Therefore the supramolecular chirality produced from achiral building blocks has become one of the attractive research fields and has been paid much attention in recent years. Up to now, several preferred methods such as chiral solvation,[2] circularly polarized light (CPL),[3] interfacial interaction[4] and gelation[5] has

been successfully employed to produce supramolecular chirality from achiral building blocks. Among these strategies, chiral solvation has been receiving intense interests due to its facility in controlling over helix sense and chirality inversion of the well–organized supramolecular structures.[2]

Supramolecular chirality in polymer structure is a fascinating interdisciplinary research area, combining the advantages of supramolecular chirality and polymers.[1a–c,1i] The supramolecular chirality in polymer can be built by assembly of main–chain or side–chain chiral/achiral polymers.[1a,6] The latter can avoid tedious and costly design and synthesis of chiral monomers or catalysts for preparing chiral polymers. To date, CPL,[7] chiral solvation[1a,6d,8] and asymmetric reaction field[9] have been successfully used to induce supramolecular chirality in polymer systems. The chiral solvation showed convincing skills in inducing supramolecular chirality in polymers, including poly(*n*–hexyl isocyanate),[8a–c] polysilanes,[8d,10a,10b] oligo(*p*–phenylenevinylene),[2g] polyfluorene analogs[10c–i] and polyacetylenes.[10k–l] However, one chiral solvent is not always effective for inducing the supramolecular chirality of all the achiral polymers, meaning the chiral solvents have to be judiciously selected for introducing supramolecular chirality into achiral polymers. Our previous results indicated that the polymer backbone structure obviously affected the induction

Suzhou Key Laboratory of Macromolecular Design and Precision Synthesis, Jiangsu Key Laboratory of Advanced Functional Polymer Design and Application, College of Chemistry, Chemical Engineering and Materials Science, Soochow University, Suzhou Industrial Park, Suzhou 215123, China. E-mail: weizhang@suda.edu.cn
†Dr. Lu Yin, Dr. Yin Zhao, Dr. Shunqin Jiang, Dr. Laibing Wang, Prof. Zhengbiao Zhang, Prof. Jian Zhu, Prof. Wei Zhang and Prof. Xiulin Zhu
Electronic Supplementary Information (ESI) available: [The GPC curves, ^{1}H NMR, UV–vis and CD spectra of star PAzoMAs. See DOI: 10.1039/x0xx00000x

of supramolecular chirality in achiral π−conjugated polymers in CHCl$_3$/limonene/CH$_3$OH tersolvents.[10i]

It is well known that azobenzene (Azo) polymers are very promising materials in the field of reversible photo-switchable materials.[11] The induction of chirality to Azo polymer is a versatile approach to construct chiroptical switches due to the dramatic changes in polarity, shape and size of Azo units, resulting in the reversible changes in UV−vis and circular dichroism (CD) spectra.[12] Recently, this concept was introduced to chiral solvation induced supramolecular chirality of achiral π−conjugated main−chain[11e] and side−chain[13] Azo polymers by our group. The reversible chiral/achiral response to *trans−/cis−*Azo was found in above two achiral Azo polymer systems.[11e,13] The chirality of side−chain Azo polymers is from the well−organized supramolecular structure of Azo units in polymer structure. On the other hand, star polymers have some unique properties compared to the their respective linear counterparts, for instance, decreased chain entanglement, lower intrinsic viscosity, reduced hydrodynamic volume and resembling more closely the hard sphere model.[14] These unique features of star polymers encourage us to study the chiral behaviours of achiral star Azo polymers induced by chiral solvation, which has never been reported previously.

Herein we reported the first generation of supramolecular chirality of star side−chain Azo polymers in aggregation state employing chiral limonene as the inducer. As compared with linear Azo polymers, several interesting results were obtained. (i) The molecular weights of 3−armed Azo polymers apparently affected their chiral assembly properties in 1,2−dichloroethane−limonene mixed solvent; (ii) Chiral amplification phenomenon is found in both 4− and 6−armed structures, but absent in linear and 3−armed polymers; (iii) The 3−armed structure with much longer side−chain presents much better fatigue durability for chiroptical switch.

Experimental section

Materials. 1-Chloro-6-hydroxyhexane (Acros, 95%), 1-chloro-11-hydroxyhexane (Acros, 95%), methacryloyl chloride (Aladdin, 95%), 4-aminoanisole (Aladdin, AR), 4-nitrophenol (Aladdin, AR), 1,1,4,7,10,10-hexamethyltriethylenetetramine (HMTETA) (Aldrich, 97%), (*R*)-(+)-limonene (1*R*, TCI, >95%, [α]$^{24}_{589}$ = +99.62°) and (*S*)-(-)-limonene (1*S*, TCI, >95%, [α]$^{24}_{589}$ = -97.72°) were used as received. Copper (I) bromide (CuBr, Aldrich, 98%) was purified with glacial acetic acid and washed with pure ethanol, then stored under argon before use. 1,2-Dichloroethane (DCE) was distilled prior to use. Unless otherwise specified, all the other chemicals were purchased from Shanghai Chemical Reagents Company (China) and used as received. The monomers, 6-[4-(4-methoxyphenylazo) phenoxy] hexyl methacrylate (AzoMA$_6$) and 11-[4-(4-methoxyphenylazo) phenoxy] undecyl methacrylate (AzoMA$_{11}$), were synthesized according to the previously reported procedures.[15] The tri−, tetra− and hexa−functional initiators (I-3Br, I-4Br and I-6Br) were synthesized according to the literature procedures via the esterification reaction between respective dolichol and 2-bromoisobutyryl bromide (Scheme S1).[15] ^{1}H NMR (CDCl$_3$, 400 MHz), (δ, ppm), I-3Br (Fig. S1a): 4.17 (s, 6H, -COOCH$_2$-), 1.94 (s, 18H, -

C(CH$_3$)$_2$-Br), 1.17 (s, 3H, -CH$_3$). Elemental analysis, calculated values for C$_{17}$H$_{27}$Br$_3$O$_6$ (%): C 36.00, H 4.80, found: C 35.71, H 4.72. I−4Br (Fig. S1b): 4.17 (s, 8H, -COOCH$_2$-), 1.94 (s, 24H, -C(CH$_3$)$_2$-Br). Elemental analysis, calculated values for C$_{21}$H$_{32}$Br$_4$O$_8$ (%): C 34.85, H 4.44, found: C 34.65, H 4.41. I−6Br (Fig. S1c): 4.17 (s, 12H, -COOCH$_2$-), 3.58 (s, 4H, -OCH$_2$-O-CH$_2$-), 1.94 (s, 36H, -C(CH$_3$)$_2$-Br). Elemental analysis, calculated values for C$_{34}$H$_{52}$Br$_6$O$_{13}$ (%): C 35.57, H 4.56, found: C 35.81, H 4.61. Preparation and isomerization of the optically active polymer aggregates was carried out according to literature procedures.[13]

Synthesis of star poly(6-[4-(4-methoxyphenylazo) phenoxy] hexyl methacrylate (SPAzoMA$_6$). 3−Armed PAzoMA$_6$ ((PAzoMA$_6$)$_{3-1}$) was prepared as follows. AzoMA$_6$ (1.0 g, 2.53 mmol), I-3Br (113.4 mg, 0.20 mmol), CuBr (56.7 mg, 0.40 mmol), HMTETA (92.3 mg, 0.40 mmol) and anisole (6.66 mL) were added successively into a 10 mL ampoule bottle. After degassing with three freeze-thaw cycles, the tube was sealed under an argon atmosphere. The polymerization was carried out at 80 ^{o}C for 12 h. It was then diluted with 2 mL THF and passed through a column of neutral alumina to remove the catalyst. After precipitation by adding the polymer solution of THF into methanol, the polymer was collected by filtration and then dried in a vacuum oven overnight at 30 ^{o}C (0.86 g, 86.0%). The 3−Armed PAzoMA$_6$s ((PAzoMA$_6$)$_{3-2}$ and (PAzoMA$_6$)$_{3-3}$) with other two different molecular weights and (PAzoMA$_{11}$)$_3$, 4−armed PAzoMA$_6$ ((PAzoMA$_6$)$_4$) and 6−armed PAzoMA$_6$ ((PAzoMA$_6$)$_6$) were prepared using the similar procedures. The molecular weights and molecular weight distributions of the obtained star polymers were listed in Table 1.

Characterization. Gel−permeation chromatography (GPC) measurements were conducted on a Waters 1515 gel permeation chromatograph (GPC) equipped with a refractive−index detector (Waters 2412), using HR1 (pore size: 100 Å, 100–5000 Da), HR2 (pore size: 500 Å, 500–20 000 Da), and HR4 (pore size 10 000 Å, 50–100 000 Da) columns (7.8 × 300 mm, 5 μm beads size) with molecular weights ranging from 10^2 ~ 5 × 10^5 g/mol. THF was used as the eluent with a flow rate of 1.0 mL/min at 40 ^{o}C. The GPC samples were injected using a Waters 717 plus autosampler and calibrated with PMMA standards from Waters. Transmission electron micrograph (TEM) images were taken with a HITACHI HT7700 operated at an accelerating voltage of 150 kV. ^{1}H NMR spectra were recorded on an INOVA 400 MHz nuclear magnetic resonance (NMR) instrument using CDCl$_3$ as the solvent and tetramethylsilane (TMS) as the internal standard at 25 ^{o}C. Elemental analyses (C, H and N) were recorded with an EA1110 CHNO−S instrument. The UV−vis spectra were measured on a UV−2600 spectrophotometer (Shimadzu (Nakagyo−ku, Kyoto, Japan)). The CD spectra were recorded on a JASCO J−815 spectropolarimeter equipped with a Peltier−controlled housing unit using a SQ−grade cuvette, with a path length of 10 mm, a scanning rate of 100 nm/min, a bandwidth of 2 nm and a response time of 1 s, using a single accumulation at 25 ^{o}C. The magnitude of the circular polarization at the ground state is defined as g_{CD} = 2 × (ε_L−ε_R)/(ε_L+ε_R), where ε_L and ε_R denote the extinction coefficients for left and right circularly polarized light, respectively. Experimentally, g_{CD} value is defined as Δε/ε = [ellipticity/32,980]/absorbance at the CD extremum.

ARTICLE

Results and discussion

Synthesis and characterization of star Azo polymers

In order to study the chiral assembly behaviours of star Azo side–chain polymers, a series of star–shaped Azo side–chain polymers with 3, 4 and 6 arms were synthesized by atom transfer radical polymerization (ATRP) initiated by tri–, tetra– and hexa–functional initiators (I–3Br, I–4Br and I–6Br) respectively (Schemes 1 and S1).[13,15] As presented in Table 1 and Fig. S2, three 3–armed Azo polymers ($(PAzoMA_6)_{3-1}$, $(PAzoMA_6)_{3-2}$ and $(PAzoMA_6)_{3-3}$) with different molecular weights (5300, 8100 and 11400 g/mol) and relatively narrow M_w/M_n (1.16–1.18) were successfully obtained via I–3Br initiated ATRP of $AzoMA_6$. Meanwhile one 3–armed Azo polymer ($(PAzoMA_{11})_3$) with relatively longer side chain (M_n = 13300 g/mol, M_w/M_n = 1.13) was achieved. Similarly, the 4– and 6–armed star Azo polymers ($(PAzoMA_6)_4$ and $(PAzoMA_6)_6$) were obtained with controlled molecular weights (10400 and 10500 g/mol) and narrow M_w/M_n values (1.13 and 1.11). The difference between $M_{n(th)}$ and $M_{n(GPC)}$ values of 4– and 6–armed polymers is attributed to the different hydrodynamic volumes of the star structures compared with the linear PMMA standards, which is not apparent in case of 3–armed structure due to its unobvious effect.[14,16] It is noteworthy that $M_{n(NMR)}$ values of all polymers agree well with those of $M_{n(th)}$, indicating a well–controlled behaviour of this polymerization.

Table 1 Molecular weight characteristics of star PAzoMAs.

Entry	Conv[a] (%)	$M_{n(th)}$[b] (g/mol)	$M_{n(GPC)}$[c] (g/mol)	M_w/M_n[d]	$M_{n(NMR)}$[e] (g/mol)
$(PAzoMA_6)_{3-1}$	86.0	4800	5300	1.18	5300
$(PAzoMA_6)_{3-2}$	77.3	8200	8100	1.16	8800
$(PAzoMA_6)_{3-3}$	72.3	14800	11400	1.18	17500
$(PAzoMA_{11})_3$	80.1	19200	13300	1.13	19200
$(PAzoMA_6)_4$	79.7	16500	10400	1.13	19400
$(PAzoMA_6)_6$	82.1	17400	10500	1.11	16200

Polymerization ratio: $[monomer]_0/[I]_0/[CuBr]_0/[HMTETA]_0$ = 12.5/1/2/2 for $(PAzoMA_6)_{3-1}$, 25/1/2/2 for $(PAzoMA_6)_{3-2}$, 50/1/2/2 for $(PAzoMA_6)_{3-3}$, $(PAzoMA_{11})_3$, $(PAzoMA_6)_4$ and $(PAzoMA_6)_6$. [a]Determined gravimetrically. [b]Caculated by $M_{n(th)}$ = $([Monomer]_0/[I]_0) \times M_{w,Monomer} \times$ conversion%. [c,d]Determined by GPC according to PMMA standards in THF. [e]$M_{n(NMR)}$ was obtained as described in Fig. S3.
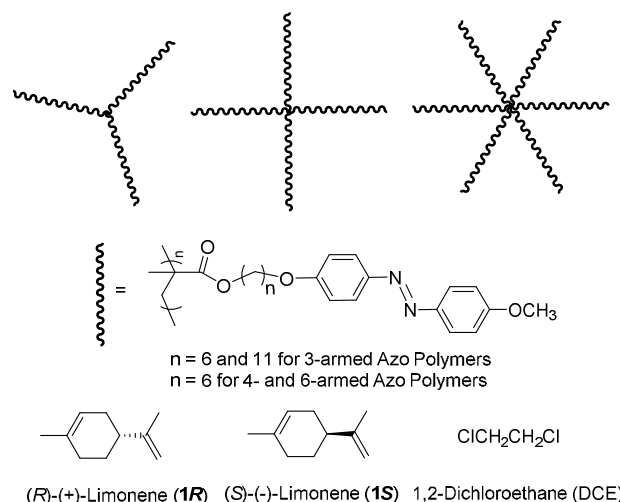
Scheme 1. Illustration of chemical structures of star Azo polymers, (R)-(+)-limonene (1R), (S)-(-)-limonene (1S) and 1,2-dichloroethane (DCE).

Effect of molecular weight and arm number of the star polymers on chiroptical property

Our previous study demonstrated that enantiomerically pure limonene played a dual role in inducing supramolecular chirality of linear PAzoMA, acting both as a chiral inducer and poor solvent meantime.[13] Moreover the choice of good solvent is also a key point for producing optically active polymer aggregates.[10c–i,13,16] In current study, 1,2-dichloroethane (DCE) and limonene (1R and 1S in Scheme 1) were also used as good solvent, and coinstantaneous chiral solvent and poor solvent because of their commercial availability, good stability and nontoxicity. It is noticeable that the volume fraction of poor solvent is vital for chiral aggregation of achiral polymers induced by chiral solvation.[10c–i,13] Higher or lower content of poor solvent will result in appearance of precipitation or weak and futile aggregation. Therefore the effect of DCE/(1R or 1S) volume ratios on chiroptical properties of all the polymers obtained with different molecular weights and different arm numbers (Table 1) was firstly studied.

As presented in Fig. S4, all the polymer aggregates in DCE/(1R or 1S) show two absorption bands (300–425 nm and 425–550 nm), owing to the π–π^* electronic transition of the *trans* isomer and n–π^* electronic transition of the *cis* isomer of Azo units in polymer side chains. Meanwhile UV–vis spectra of all the polymers show the similar gradually declining and broadening trend with the increase of limonene volume fraction in mixed solvents, exhibiting an apparent organization of Azo units via π–π stacking.[13] Appearance of a UV shoulder band at 342 nm at relatively low volume ratio of DCE/(1R or 1S) indicated that Azo stacks preferred H–aggregates in DCE/(1R or 1S).

Circular dichroism (CD) spectra (Figs. 1a-f) showed very strong mirror image Cotton effects, demonstrating that the chiral solvation successfully induced the helical π–stacks of Azo units in all the polymer side chains with preferred handedness

under the optimized DCE/(1R or 1S) volume ratios. Three 3−armed Azo polymers ((PAzoMA$_6$)$_3$s in Table 1) with different M_ns (5300, 8100 and 11400 g/mol) were employed to study the effects of molecular weights on the chirality induction from chiral limonene. Figs. 1a–c, 1g and 1i presented a similar changing tendency of maximum CD (Figs. 1g and 1h) and g_{CD} values with DCE/(1R or 1S) volume ratios for each polymer, similar to that of linear counterpart reported previously.[13] The maximum CD (Figs. 1g and 1h) and g_{CD} (Figs. 1i and 1j) values of each polymer aggregates both increased gradually with the relative DCE/(1R or 1S) (v/v) value, then decreased steeply after obtaining their maximum values. Interestingly, the DCE/(1R or 1S) (v/v) value at the maximum CD (Figs. 1g and 1h) and g_{CD} value positions (DCE/1R = 0.2/2.8, 0.4/2.6, 0.6/2.4 and DCE/1S = 0.25/2.75, 0.4/2.6, 0.5/2.5 for (PAzoMA$_6$)$_{3-1}$, (PAzoMA$_6$)$_{3-2}$ and (PAzoMA$_6$)$_{3-3}$ respectively, v/v) increased with polymer molecular weights, implying that much longer chain length need much more good solvent for ideal chiral aggregation because of its relatively poor solubility in same mixed solvents. More interestingly, the enhancement of the absolute maximum CD (Figs. 1g and 1i) and g_{CD} (Figs. 1h and 1j) values are distinct with polymer molecular weights under optimized conditions, for instance they increased from 25.7 (CD) and 6.1 × 10^{-4} (g_{CD}) to 44.2 (CD) and 8.9 × 10^{-4} (g_{CD}) for DCE/1R, and from 24.9 (CD) and 4.9 × 10^{-4} (g_{CD}) to 39.4 (CD) and 8.4 × 10^{-4} (g_{CD}) for DCE/1S, respectively. The reason may be that the preferred-handed helical structure with much more Azo units should be contained in relatively longer polymer chain, resulting in corresponding higher maximum CD (Figs. 1g and 1h) and g_{CD} (Figs. 1i and 1j) values.[17] However, the absolute maximum CD (Fig. 1h) and g_{CD} (Fig. 1j) values of (PAzoMA$_{11}$)$_3$ showed much feeble dependence on DCE/(1R or 1S) volume ratio than those of other 3−armed Azo polymers with relatively short side chains. It is because that the longer side chain will result in much better solubility of polymer in the same mixed solvents, providing more sufficient mobility for the stacking of Azo units.

The effect of arm number on the chiral assembly behaviour of polymer under different DCE/(1R or 1S) (v/v) conditions was further studied and the results were given in Fig. 1. Remarkably the absolute maximum CD (Figs. 1g and 1h) and g_{CD} (Figs. 1i and 1j) values of polymer aggregates increased with the number of arms (3−arm < 4−arm < 6−arm) under the respective optimized condition. The absolute maximum CD (Figs. 1a and 1b) values are 44.2, 45.2 and 50.4 (DCE/1R), and 39.4, 49.5 and 50.5 (DCE/1S) for (PAzoMA$_6$)$_{3-3}$, (PAzoMA$_6$)$_4$ and (PAzoMA$_6$)$_6$ aggregates respectively. Meanwhile the absolute maximum g_{CD} (Figs. 1i and 1j) values for above polymer aggregates are 8.9 × 10^{-4}, 9.1 × 10^{-4} and 1.2 × 10^{-3} (DCE/1R), and 8.4 × 10^{-4}, 1.1 × 10^{-3} and 1.3 × 10^{-3} (DCE/1S). On the other hand, the DCE/(1R or 1S) (v/v) value at the maximum CD (Figs. 1g and 1h) and g_{CD} (Figs. 1i and 1j) value positions (DCE/1R = 0.6/2.4, 0.5/2.5, 0.3/2.7 and DCE/1S = 0.5/2.5, 0.5/2.5, 0.3/2.7 for (PAzoMA$_6$)$_{3-3}$, (PAzoMA$_6$)$_4$ and (PAzoMA$_6$)$_6$ respectively, v/v) slightly increased with the arm numbers of the polymers. The possible reasons responsible for the above results may be the increased segmental density and decreased intrinsic viscosity

with an increasing numbers of arms in the star polymers.[14] These new findings will pave the way for producing the chiral materials with high CD and g_{CD} values.
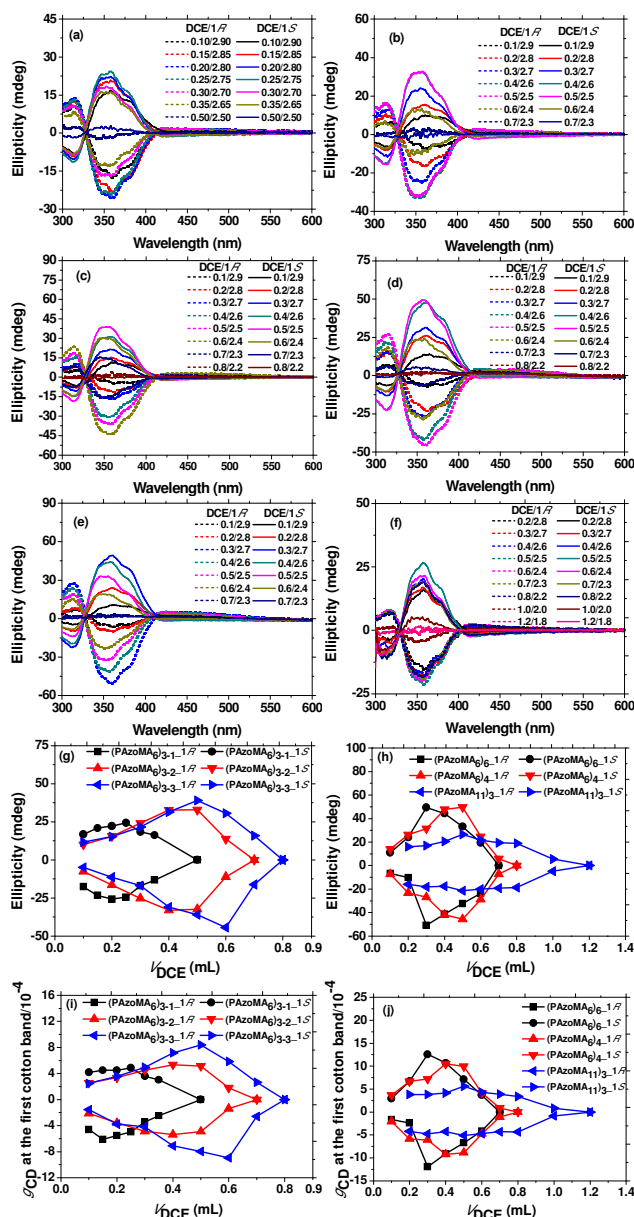

Fig. 1 Circular dichroism (CD) spectra of PAzoMA aggregates in mixed solvents with different DCE/(1R or 1S) volume fractions. (a)-(f) stands for (PAzoMA$_6$)$_{3-1}$, (PAzoMA$_6$)$_{3-2}$, (PAzoMA$_6$)$_{3-3}$, (PAzoMA$_6$)$_4$, (PAzoMA$_6$)$_6$ and (PAzoMA$_{11}$)$_3$, respectively. The maximum CD (g, h) and g_{CD} values (i, j) (360 nm) of star Azo polymer aggregates depend on DCE/(1R or 1S) volume fractions. The concentration of polymer repeating units is 8.42 × 10^{-5} mol/L. The data in g-j were taken from a-f.

Chiral amplification

Considering the importance of chiral amplification,[18] the possibility of chiral amplification in assembly of Azo units in

star polymer chains were investigated by varying enantiomeric excess (*ee*) of chiral limonene, while keeping the total volume ratio of DCE and limonene constant. In cases of all 3–armed Azo star polymers, the linear plot of maximum CD (Fig. 2a) and g_{CD} values (Fig. 2b) at 360 nm demonstrated that the helical sense of the Azo stacks in polymer chain was controlled by the respective molar ratio of enantiomers (1*R*/1*S*), e.g., no obvious chiral amplification occurred. The similar phenomena were also found in chiral solvation induced supramolecular chirality of linear π–conjugated main–chain polymers[10c–i] and side–chain Azo polymers reported previously.[13] Amazedly the nonlinear dependence of maximum CD (Fig. 2a) and g_{CD} (Fig. 2b) values at 360 nm on *ee* of limonene was observed in case of 4–armed and 6–armed counterparts ((PAzoMA$_6$)$_4$ and (PAzoMA$_6$)$_6$). The tentative explanation is that the more compact sphere model with increasing arm numbers of star Azo polymers resulted in the chiral amplification. The real reason for this interesting results is being studied in our group. Actually it is the first unique observation of chiral amplification by the transfer of chiral information from the chiral solvation to achiral Azo stacks in polymer side chains, even though this phenomena were reported in chiral polymers[18] and oligomer systems[17a] before.
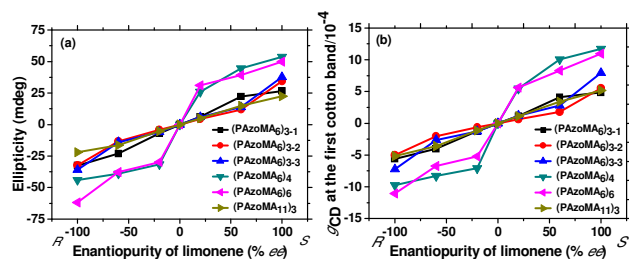

Fig. 2 Plots of maximum CD (a) and g_{CD} (b) values (360 nm) of star Azo polymer aggregates measured with different enantiopurity of limonene. DCE/(1*R* + 1*S*) are 0.25/2.75, 0.4/0.6, 0.5/2.5, 0.3/2.7, 0.5/2.5 and 0.5/2.5 (v/v) for (PAzoMA$_6$)$_{3-1}$, (PAzoMA$_6$)$_{3-2}$, (PAzoMA$_6$)$_{3-3}$, (PAzoMA$_6$)$_4$, (PAzoMA$_6$)$_6$ and (PAzoMA$_{11}$)$_3$ respectively. The concentration of polymer repeating units is 8.42 × 10^{-5} mol/L. These data were taken from Fig. S5.

Photo– and thermal isomerization of polymer aggregates

The unique *tran–cis* isomerization of Azo units endows their potential applications in light-controlled functional materials, *e.g*, shape memory, optical data storage and chiroptical switches.[11,13] Our previous study showed that *tran–cis* photoisomerization of Azo linear polymer could easily occur in aggregation state.[13] Similarly, the *tran–cis* photoisomerization of Azo star polymers in aggregation state was also investigated. As displayed in Figs. 3 (a and b) and S6, the decrease of the characteristic π–π* transition of *trans*–Azo at around 360 nm, accompanying the increase of *n*–π* transition of *cis*–Azo at around 453 nm, demonstrating the successful *tran–cis* photoisomerization triggered by 365 nm light irradiation. The inverse change of UV–vis spectra of Azo star polymers aggregates by irradiated by 436 nm light proved the occurrence of *cis–tran* photoisomerization. This reversible photoisomerization process can be cycled by 365/436 nm light alternating irradiation. The thermal

isomerization is an alternative way to perform *cis–trans* transformation of Azo units owing to its low activation energy. Expectedly, the stepwise decrease of the absorption at around 453 nm (typical *n*–π* electronic transition of *cis*–isomer) and the gradual increase of the absorption near 360 nm (typical π–π* electronic transition of *trans*–isomer) (Figs. 3 (c and d) and S7) with heating time indicated the performance of *cis–trans* isomerization, which reached stable state within 40 min at 60 °C. Furthermore, the recovered absorption intensity at around 360 nm was a little higher than the original value, demonstrating the higher relative content of *tran*–isomer after the thermal isomerization.
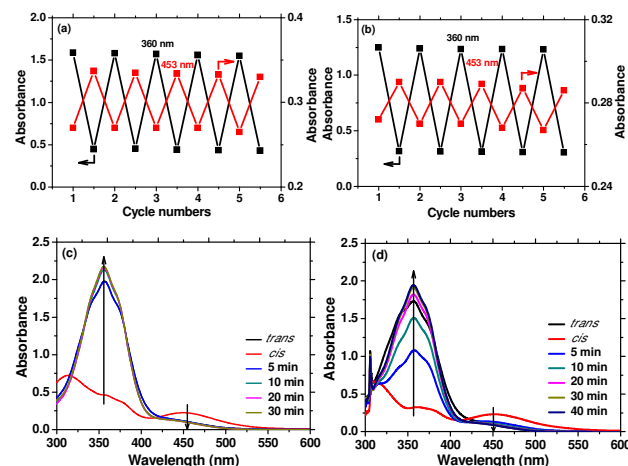

Fig. 3 Photo– and thermal isomerization of (PAzoMA$_6$)$_{3-1}$ aggregates (a and c) DCE/1*R* and (b and d) DCE/1*S* by alternating irradiation with 365 nm and 436 min light for 3 min (a and b) or alternating 365 nm light irradiation for 3 min and heating at 60 °C for different time (c and d). The data in Fig. 3a and 3b were taken from Fig. S6 (1a, 1b, 1d and 1e).

Chiral switching property

The incorporation of Azo units into chiral polymer chains provides a versatile way to construct chiroptical switches due to the drastic changes of molecular shape and polarity during the *trans–cis* isomerization of Azo groups.[12] Indeed this approach need sophisticated design and tedious synthesis of chiral Azo monomers prior to polymerization, while showing lack of control over the chirality in some cases. Our previous studies demonstrated that complete conformational changes of both linear achiral main-chain[10e] and side–chain[13] Azo–containing polymers were achieved by *trans–cis* isomerization of Azo groups under chiral solvation conditions, supported by changes from intensely CD–active to completely CD–inactive states. These interesting results motivate us to study the chiroptical switching properties of current star Azo polymer systems. Similarly, the CD signals derived from the supramolecularly chiral *trans*–Azo stacks in all synthesized polymers completely disappeared in *cis*–Azo states trigged by 365 nm light irradiation for 3 min (Figs. 4 and S8), regardless of 1*R* and 1*S*. The reason is that the helical Azo stacks induced by limonene solvation was disrupted by bent-shape form of *cis*–Azo.[5f,13] Furthermore the destroyed helical sense of Azo units could not be recovered by 436 nm light irradiation (data not shown here). However it was generated by *cis–trans* thermal–isomerization

process (keeping the solution at 60 ^{o}C for 40 min and cooling down to room temperature), accompanying by an obvious ~45 nm red shift (from 360 nm to 405 nm) of CD absolute maximum position (Figs. 4 and S9). The red shift is ascribed to the relatively longer Azo stacks formed after *cis−trans* thermal−isomerization process. The possible reason is that the confined space in aggregation state hinders the reassembly of Azo units in polymer side chains during the *cis−trans* photoisomerization, as supported by the following TEM analysis (Figs. 5 and S10). However, under thermal isomerisation conditions, *i.e.*, the polymer solutions were kept 60 ^{o}C for 40 min and then cooled to room temperature, the polymer chains will become relatively flexible to reform the highly organized helical Azo stacks, as reported previously in linear Azo polymer system.[13]

It is noticeable that the molecular weights of 3−armed Azo polymers and arm numbers of polymers have an obvious effect on their chiroptical behaviours upon alternating 365 nm light irradiation and heating−cooling treatment. As presented in Figs. 4 and S9(1a−2a), the 3−armed polymer with relatively low molecular weight ((PAzoMA$_6$)$_{3-1}$, M_n = 5300 g/mol) showed better reversibility of chiral−achiral switch (even after 6 cycles) than other two polymers with higher molecular weights ((PAzoMA$_6$)$_{3-2}$, M_n = 8100 g/mol and (PAzoMA$_6$)$_{3-3}$, M_n = 11400 g/mol). The chiroptical switching ability of these polymers decreased in the order (PAzoMA$_6$)$_{3-1}$ > (PAzoMA$_6$)$_{3-2}$ > (PAzoMA$_6$)$_{3-3}$. It is because that the difficulty of repeatedly deforming and reforming the supramolecular helical structures increases with polymer chain length. Considering the similar repeating units in (PAzoMA$_{11}$)$_3$ (DP = 40) and (PAzoMA$_6$)$_{3-3}$ (DP = 42), the chiroptical switching property of the former is better than that of the latter (Figs. S9(2b) and S9(5b)), indicating the longer side−chain length provides much better reassembly ability. Meanwhile, the increased arm numbers of polymers also will decrease the reversible ability of chiroptical switches, as presented in Figs. S9.
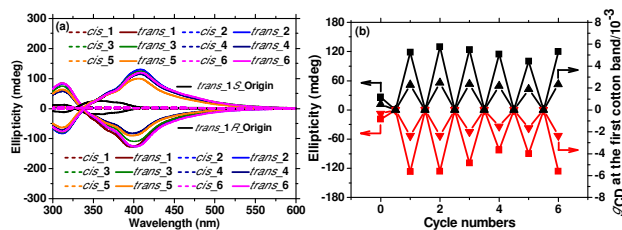

Fig. 4 Changes in CD spectra (a) and the maximum CD and g_{CD} values (b) of (PAzoMA$_6$)$_{3-1}$ aggregates in DCE/(1R or 1S) during alternating 365 nm light irradiation (3 min) and heating−cooling treatment (60 ^{o}C for 40 min then cooling to room temperature). DCE/(1R or 1S) = 0.25/2.75. The concentration of polymer repeating units is 8.42 × 10^{-5} mol/L. The data in Fig. 4b are taken from Fig. 4a.

The changes in the size and morphology of polymer aggregates were monitored by transmission electron microscope (TEM) during the process of alternating 365 nm light irradiation and heating-cooling treatment. The results were shown in Figs. 5 and S10. In case of (PAzoMA$_6$)$_{3-1}$ in DCE/1R, the initial polymer aggregates is composed of irregular nanoparticles. The aggregates changed to relatively regular nanoparticles with about 1000 nm in diameter after 365 nm light (irradiation for 3 min) induced *trans−cis* isomerization. The deformation of the well−organized Azo stacks occurred under 365 nm light irradiation, while these Azo polymers simultaneously re−assembly into bigger aggregates containing more polymer chains. This observation supported the corresponding disappearance of CD signals as mentioned above. The particles with relatively small sizes (340 nm and 115 nm in diameter) were observed after heating−cooling treatment. The reason may be that the cooling speed is too fast to provide sufficient time to form the aggregates with uniform sizes. The difference of the morphology and size of polymer aggregates between the original sample and the sample after *trans−cis−trans* cycle may result in the red shift in CD spectra (Fig. 4a). Furthermore the 1350 nm size particles were formed (Fig. 5d) when the above polymer aggregates were irradiated with 365 nm light for 3 min again. Similar results were also obtained when 1R was replaced by 1S (Fig. 5e−h). Other polymer aggregates demonstrate the similar results under identical conditions as presented in Fig. S10.
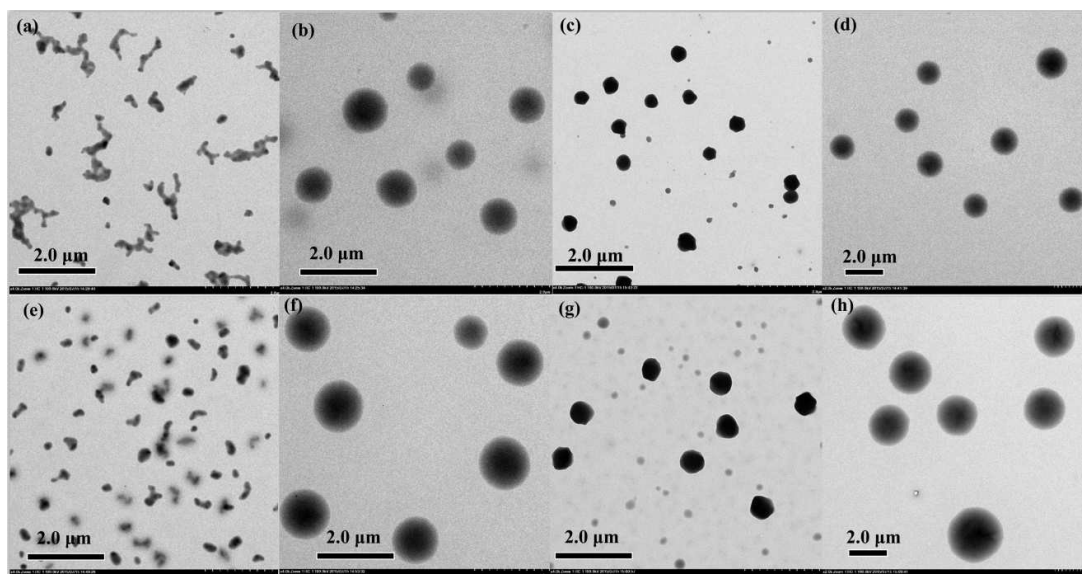
Fig. 5 TEM images of (PAzoMA$_6$)$_{3-1}$ aggregates during chiroptical switching process. (a–d for DCE/1*R* and e–h for DCE/1*S*). The original *trans*–form (a and e), after the first 3 min 365 nm light irradiation (b and f), after the heating–cooling treatment (c and g), after the second 3 min 365 nm light irradiation (d and h).

Conclusions

The supramolecular chirality was successfully introduced to achiral star Azo side–chain polymer systems induced by chiral solvation of limonene. This chirality is from the helical sense of Azo stacks formed in polymer side chain in DCE/limonene mixed solvent. The absolute maximum CD and g_{CD} values of the polymer aggregates increased with the molecular weight of the 3–armed polymers, and increased with the arm numbers of the polymers within the similar molecular weights. The chiral amplification phenomena were observed for the first time in 4– and 6–armed polymer systems. The polymer with lower molecular weight and less arm numbers demonstrates the preferable chiral switching ability upon alternating 365 nm light irradiation and heating–cooling treatment.

Acknowledgements

Notes and references

1   (a) J. J. L. M. Cornelissen, A. E. Rowan, R. J. M. Nolte and N. A. J. M. Sommerdijk, *Chem. Rev.*, 2001, **101**, 4039; (b) G. A. Hembury, V. V. Borovkov and Y. Inoue, *Chem. Rev.*, 2008, **108**, 1; (c) T. F. A. de Greef, M. M. J. Smulders, M. Wolffs, A. P. H. J. Schenning, R. P. Sijbesma and E. W. Meijer, *Chem.*

Rev., 2009, **109**, 5687; (d) A. Scarso and J. J. Rebek, *Top. Curr. Chem.*, 2006, 265, 1; (e) R. Oda, I. Huc, M. Schmutz, S. J. Candau and F. C. MacKintosh, *Nature*, 1999, **399**, 566; (f) H. Engelkamp, S. Middelbeek and R. J. M. Nolte, *Science*, 1999, 284, 785; (g) A. E. Rowan and R. J. M. Nolte, *Angew. Chem. Int. Ed.*, 1998, **37**, 63; (h) J. C. Nelson, J. G. Saven, J. S. Moore and P. G. Wolynes, *Science*, 1997, **277**, 1793; (i) M. H. Liu, L. Zhang and T. Y. Wang, *Chem. Rev.*, DOI: 10.1021/cr500671p.

2   (a) C. C. Lee, C. Grenier, E. W. Meijer and A. P. H. J. Schenning. *Chem. Soc. Rev.*, 2009, **38**, 671; (b) H. von Berlepsch, S. Kirstein and C. Böttcher. *J. Phys. Chem. B*, 2003, **107**, 9646; (c) S. Ghosh, X. Q. Li, V. Stepanenko and F. Würthner, *Chem. Eur. J.*, 2008, **14**, 11343; (d) J. Aimi, Y. Nagamine, A. Tsuda, A. Muranaka, M. Uchiyama and T. Aida. *Angew. Chem. Int. Ed.*, 2008, **47**, 5153; (e) B. Isare, M. Linares, L. Zargarian, S. Fermandjian, M. Miura, S. Motohashi, N. Vanthuyne, R. Lazzaroni and L. Bouteiller, *Chem. Eur. J.*, 2010, **16**, 173; (f) S. J. George, R. de Bruijn, Ž. Tomović, B. V. Averbeke, D. Beljonne, R. Lazzaroni, A. P. H. J. Schenning and E. W. Meijer, *J. Am. Chem. Soc.*, 2012, **134**, 17789; (g) S. J. George, Ž. Tomović, A. P. H. J. Schenning and E. W. Meijer, *Chem. Commun.*, 2011, **47**, 3451; (h) W. Zhang, M. Fujiki and X. L. Zhu, *Chem. Eur. J.*, 2011, **17**, 10628.

3   (a) O. Buchardt, *Angew. Chem. Int. Ed.*, 1974, **13**, 179; (b) F. Vera, R. M. Tejedor, P. Romero, J. Barberá, M. B. Ros, J. L. Serrano and T. Sierra, *Angew. Chem. Int. Ed.*, 2007, **46**, 1873; (c) S. T. Wu, Z. W. Cai, Q. Y. Ye, C. H. Weng, X. H. Huang, X. L. Hu, C. C. Huang and N. F. Zhuang, *Angew. Chem. Int. Ed.*, 2014, **53**, 12860.

4   (a) J. Yuan and M. H. Liu, *J. Am. Chem. Soc.*, 2003, **125**, 5051; (b) P. Z. Guo and M. H. Liu, *Langmuir*, 2005, **21**, 3410; (c) Z. X. Guo, J. Yuan, Y. Cui, F. Chang, W. H. Sun and M. H. Liu, *Chem. Eur. J.*, 2005, **11**, 4155; (d) Y. F. Qiu, P. L. Chen, P. Z. Guo, Y. G. Li and M. H. Liu, *Adv. Mater.*, 2008, **20**, 2908; (e) P. L. Chen, X. G. Ma, K. M. Hu, Y. L. Rong and M. H. Liu, *Chem. Eur. J.*, 2011, **17**, 12108.

5   (a) S. Y. Zhang, S. Y. Yang, J. B. Lan, S. J. Yang and J. S. You, *Chem. Commun.*, 2008, 6170; (b) P. F. Duan, H. Cao, L. Zhang and M. H. Liu, *Soft Matter*, 2014, **10**, 5428; (c) L. Zhang, X. F. Wang, T. Y. Wang and M. H. Liu, *Small*, **11**, 1025; (d) Y. G. Li

and M. H. Liu, *Chem. Commun.*, 2008, 5571; (e) Z. C. Shen, T. Y. Wang, L. Shi, Z. Y. Tang and M. H. Liu, *Chem. Sci.*, 2015, **6**, 4267; (f) J. Wang, G. Yang, H. Jiang, G. Zou and Q. J. Zhang, *Soft Matter*, 2013, **9**, 9785.

6   (a) P. Pino and G. P. Lorenzi, *J. Am. Chem. Soc.*, 1960, **82**, 4745; (b) E. Yashima, T. Matsushima and Y. Okamoto, *J. Am. Chem. Soc.*, 1995, **117**, 11596; (c) E. Yashima and K. Maeda, *Macromolecules*, 2008, **41**, 3; (d) E. Yashima, K. Maeda, H. Iida, Y. Furusho and K. Nagai, *Chem. Rev.*, 2009, **109**, 6102.

7   (a) L. Nikolova, T. Todorov, M. Ivanov, F. Andruzzi, S. Hvilsted and P. S. Ramanujam, *Opt. Mater.*, 1997, **8**, 255; (b) S.-W. Choi, S. Kawauchi, N. Y. Ha and H. Takezoe, *Phys. Chem. Chem. Phys.*, 2007, **9**, 3671; (c) Y. Wang, T. Sakamoto and T. Nakano, *Chem. Commun.*, 2012, **49**, 1871; (d) M. Fujiki, K. Yoshida, N. Suzuki, J. Zhang, W. Zhang and X. L. Zhu, *RSC Adv.*, 2013, **3**, 5213; (e) Y. Y. Xu, G. Yang, H. Y. Xia, G. Zou, Q. J. Zhang and J. G. Gao, *Nat. Commun.*, 2014, **5**, 5050; (f) M. Fujiki, Y. Donguri, Y. Zhao, A. Nakao, N. Suzuki, K. Yoshida and W. Zhang, *Polym. Chem.*, 2015, **6**, 1627.

8   (a) M. M. Green, C. Khatri and N. C. Peterson, *J. Am. Chem. Soc.*, 1993, **115**, 4941; (b) M. M. Green, J. W. Park, T. Sato, A. Teramoto, S. Lifson, R. L. B. Selinger and J. V. Selinger, *Angew. Chem. Int. Ed.*, 1999, **38**, 3138; (c) M. Fujiki, *Symmetry*, 2014, **6**, 677; (d) H. Nakashima, J. R. Koe, K. Torimitsu and M. Fujiki, *J. Am. Chem. Soc.*, 2001, **123**, 4847.

9   (a) M. Goh, S. Matsushita and K. Akagi, *Chem. Soc. Rev.*, 2010, **39**, 2466; (b) A. Akagi, *Chem. Rev.*, 2009, **109**, 5354; (c) M. Goh, M. Kyotani and K. Akagi, *J. Am. Chem. Soc.*, 2007, **129**, 8519; (d) J. Park, T. J. Yu, T. Inagaki and K. Akagi, *Macromolecules*, 2015, **48**, 1930.

10 (a) P. Dellaportas, R. G. Jones and S. J. Holder, *Macromol. Rapid Commun.*, 2002, **23**, 99; (b) Y. Nakano, F. Ichiyanagi, M. Naito, Y. G. Yang and M. Fujiki, *Chem. Commun.*, 2012, **48**, 6636; (c) Y. Nakano, Y. Liu and M. Fujiki, *Polym. Chem.*, 2010, **1**, 460; (d) Y. Kawagoe, M. Fujiki and Y. Nakano, *New J. Chem.*, 2010, **34**, 637; (e) W. Zhang, K. Yoshida, M. Fujiki and X. L. Zhu, *Macromolecules*, 2011, **44**, 5105; (f) M. Fujiki, A. J. Jalilah, N. Suzuki, M. Taguchi, W. Zhang, M. M. Abdellatif and K. Nomura, *RSC Adv.*, 2012, **2**, 6663; (g) S. S. Zhang, J. F. Liu, J. Zhang, L. B. Wang, W. Zhang and X. L. Zhu, *Acta Polym. Sin.*, 2013, **4**, 426; (h) J. F. Liu, J. Zhang, S. S. Zhang, N. Suzuki, M. Fujiki, L. B. Wang, L. Li, W. Zhang, N. C. Zhou and X. L. Zhu, *Polym. Chem.*, 2014, **5**, 784; (i) L. B. Wang, N. Suzuki, J. F. Liu, T. Matsuda, N. A. A. Rahim, W. Zhang, M. Fujiki, Z. B. Zhang, N. C. Zhou and X. L. Zhu, *Polym. Chem.*, 2014, **5**, 5920; (j) D. Lee, Y. J. Jin, H. Kim, N. Suzuki, M. Fujiki, T. Sakaguchi, S. K. Kim, W. E. Lee and G. Kwak, *Macromolecules*, 2012, **45**, 5379; (k) H. Kim, D. Lee, S. Lee, N. Suzuki, M. Fujiki, C.-L. Lee and G. Kwak, *Macromol. Rapid Commun.*, 2013, **34**, 1471; (l) H. Kim, Y.-J. Jin, B. S. Kim, T. Aoki, G. Kwak, *Macromolecules*, 2015, DOI: 10.1021/acs.macromol.5b01034.

11 (a) A. Natansohn and P. Rochon, *Chem. Rev.*, 2002, **102**, 4139; (b) D. R. Wang and X. G. Wang, *Prog. Polym. Sci.*, 2013, **38**, 271; (c) Y. Zhao and J. He, *Soft. Matter.*, 2009, **5**, 2686; (d) Y. L. Yu, M. Nakano and T. Ikeda, *Nature*, 2003, **425**, 145; (e) Wang, W.; Sun, X. M.; Wu, W.; Peng, H. S.; Yu, Y. L. *Angew. Chem. Int. Ed.*, 2012, **51**, 4644; (f) L. B. Wang, X. Q. Pan, Y. Zhao, Y. Chen, W. Zhang, Y. F. Tu, Z. B. Zhang, J. Zhu, N. C. Zhou and X. L. Zhu. *Macromolecules*, 2015, **48**, 1289.

12 (a) S. R. Lustig, G. J. Everlof and G. D. Jaycox, *Macromolecules*, 2001, **34**, 2364; (b) A. Bobrovsky, V. Shibaev, A. Bubnov, V. Hamplová, M. Kašpar and M. Glogarová, *Macromolecules*, 2013, **46**, 4276; (c) H. Sogawa, M. Shiotsuki and F. Sanda, *Macromolecules*, 2013, **46**, 4378; (d) S. Leclair, L. Mathew, M. Giguère, S. Motallebi and Y. Zhao, *Macromolecules*, 2003, **36**, 9024.

13 S. Q. Jiang, Y. Zhao, L. B. Wang, L. Yin, Z. B. Zhang, J. Zhu, W. Zhang and X. L. Zhu, *Polym. Chem.*, 2015, **6**, 4230.

14 (a) L. J. Fetters, A. D. Kiss, D. S. Pearson, G. F. Quack and F. J. Vitus, *Macromolecules*, 1993, **26**, 647; (b) K. Shida, K. Ohno, M. Kimura, Y. Kawazoe and Y. Nakamura, *Macromolecules*, 1998, **31**, 2343; (c) R. M. England and S. Rimmer, *Polym. Chem.*, 2010, **1**, 1533.

15 (a) Y. Y. Zhang, W. Zhang, X. R. Chen, Z. P. Cheng, J. H. Wu, J. Zhu and X. L. Zhu, *J. Polym. Sci., Part A: Polym. Chem.*, 2008, **46**, 777; (b) G. Wang, X. Tong and Y. Zhao, *Macromolecules*, 2004, **37**, 8911.

16 (a) J. Z. Liu, H. M. Su, L. M. Meng, Y. H. Zhao, C. M. Deng, J. C. Y. Ng, P. Lu, M. Faisal, J. W. Y. Lam, X. H. Huang, H. K. Wu, K. S. Wong and B. Z. Tang, *Chem. Sci.*, 2012, **3**, 2737; (b) H. K. Li, J. Cheng, Y. H. Zhao, J. W. Y. Lam, K. S. Wong, H. K. Wu, B. S. Li and B. Z. Tang, *Mater. Horiz.*, 2014, **1**, 518.

17 (a) S. J. George, Ž. Tomović, M. M. J. Smulders, T. F. A. de Greef, P. E. L. G. Leclère, E. W. Meijer and A. P. H. J. Schenning, *Angew. Chem. Int. Ed.*, 2007, **46**, 8206; (b) T. Nakano, *Chem. Rec.*, 2014, **14**, 369.

18 (a) M. M. G, B. A. Garetz, B. Munoz, H. P. Chang, S. Hoke and R. G. Cooks, *J. Am. Chem. Soc.*, 1995, **117**, 4181; (b) Y. Nagata, T. Yamada, T. Adachi, Y. Akai, T. Yamamoto and M. Suginome, *J. Am. Chem. Soc.*, 2013, **135**, 10104; (c) M. Verswyvel and G. Koeckelberghs, *Polym. Chem.*, 2012, **3**, 3203; (d) A. R. A. Palmans and E. W. Meijer, *Angew. Chem. Int. Ed.*, 2007, **46**, 8948.

Graphical Abstract

Preferential Chiral Solvation Induced Supramolecular Chirality in Optically Inactive Star Azo Polymers: Photocontrollability, Chiral Amplification and Topological Effect

Lu Yin, Yin Zhao, Shunqin Jiang, Laibing Wang, Zhengbiao Zhang, Jian Zhu, Wei Zhang* and Xiulin Zhu
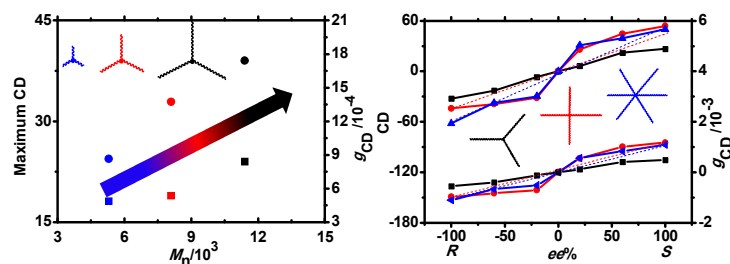
The chiral amplification phenomena were observed for the first time in 4− and 6−armed Azo star side-chain polymer systems, but absent in linear and 3−armed counterparts.